ARMY RESEARCH LABORATORY

Meteorological Data Processing Methods in the Computer-Assisted Artillery Meteorology System (Battlescale Forecast Model)

By Patrick A. Haines
Abel J. Blanco
Information Science and Technology Directorate
Battlefield Environment Division

and

S.A. Luces
John B. Spalding
Physical Science Laboratory, New Mexico State University

ARL-TR-559

July 1997

Approved for public release. Distribution is unlimited.

NOTICES

Disclaimers

The findings in this report are not to be construed as an official Department of the Army position unless so designated by other authorized documents.

The citation of manufacturer's trade names and names of manufacturers in this report is not to be construed as official Government endorsement or approval of commercial products or services rendered herein.

REPORT DOCUMENTATION PAGE

Form Approved
OMB No. 0704-0188

1. AGENCY USE ONLY (Leave Blank)	2. REPORT DATE	3. REPORT TYPE AND DATES COVERED
	July 1997	Final

4. TITLE AND SUBTITLE

Meteorological Data Processing Methods in the Computer-Assisted Artillery Meteorology System (Battlescale Forecast Model)

5. FUNDING NUMBERS

6. AUTHOR(S)

Patrick A. Haines, Abel J. Blanco, Battlefield Environment Division
S. A. Luces, and J. B. Spalding, Physical Science Laboratory

7. PERFORMING ORGANIZATION NAMES(s) AND ADDRESS(ES)

U.S. Army Research Laboratory
Information Science and Technology Directorate
Battlefield Environment Division
White Sands Missile Range, NM 88002-5501

Physical Science Laboratory
New Mexico State University
Las Cruces, NM 88003

8. PERFORMING ORGANIZATION REPORT NUMBER

ARL-TR-559

9. SPONSORING/MONITORING AGENCY NAMES(S) AND ADDRESS(ES)

U.S. Army Research Laboratory
2800 Powder Mill Road
Adelphi, MD 20783-1145

10. SPONSORING/ MONITORING AGENCY REPORT NUMBER

ARL-TR-559

11. SUPPLEMENTARY NOTES

12a. DISTRIBUTION/AVAILABILITY STATEMENT

Approved for public release; distribution unlimited.

12b. DISTRIBUTION CODE

A

13. ABSTRACT (Maximum 200 words)

The purpose of this report is to present basic information on the theoretical and practical meteorological (met) principles employed in the Computer-Assisted Artillery Meteorology (CAAM) system using the Battlescale Forecast Model (BFM). CAAM (BFM) was designed to assimilate several types of met inputs, process these data, and produce artillery met messages, all on the battlefield. Central to this system is the use of a mesoscale atmospheric prediction model (the BFM). The introduction gives a history of the program and an overview of the design of CAAM. The model domain is described in terms of an area of operations and the data required to operate the model. Model initialization in terms of a three-dimensional objective analysis is described for two modes: with and without the input from a larger scale forecast model. The methods of the BFM are described in terms of initialization, nudging to the objective analysis, and the model forecast technique. The output of CAAM consists of two kinds of artillery computer met messages; these are derived from both the objective analysis and the BFM results. Finally, future improvements are mentioned.

14. SUBJECT TERMS	15. NUMBER OF PAGES 62	
meteorological data processing, artillery meteorology	16. PRICE CODE	

17. SECURITY CLASSIFICATION OF REPORT	18. SECURITY CLASSIFICATION OF THIS PAGE	19. SECURITY CLASSIFICATION OF ABSTRACT	20. LIMITATION OF ABSTRACT
UNCLASSIFIED	UNCLASSIFIED	UNCLASSIFIED	SAR

NSN 7540-01-280-5500

Standard Form 298 (Rev. 2-89)
prescribed by ANSI Std. Z39-18 298-102

Preface

This report is intended to present basic information about the theoretical and practical principles employed in the Computer-Assisted Artillery Meteorology (CAAM) Battlescale Forecast Model (BFM) system. The purpose of CAAM is to assimilate a variety of meteorological (met) inputs in the battlefield which are used to make a forecast using a mesoscale numerical weather prediction model. The forecast, in turn, is used to produce improved artillery met messages tailored for specified gun and target locations. This report primarily addresses the met components of CAAM, but a brief history of the CAAM project and its internal organization are given in the introduction.

CAAM represents a significant step toward overcoming the "staleness" problem associated with simple use of met data. Rapidly changing weather conditions imply large spatial and temporal gradients of met fields, in which case, a single or even a few reports alone are insufficient to characterize the four-dimensional evolution of the atmosphere. Thus, a mesoscale prediction model is employed. The model begins with as accurate a portrayal of the three-dimensional atmospheric structure as is possible and then predicts its future three-dimensional structure. The resulting forecast of wind, temperature, and pressure is used to produce improved met messages not only for conventional gun/target distances, but also for distant target areas. CAAM also improves the characterization of target area meteorology which is important in estimating when and where to employ submunitions that are deployed above the target, and are therefore affected by local target, low-level conditions. CAAM (BFM) has undergone a series of modifications and improvements since its original design, and is now in version 4.

Six types of met input files are received and managed by the External Interface component. Once sufficient data are present, and the Area of Operations (AOP) has been initialized, the modeling sequence can begin. This sequence has three components which are executed in series:

- objective analysis (two possible methods),
- BFM (two possible methods), and
- met Message generation.

When the sequence is completed, two types of met messages will have been generated: the computer met message (MET-CM) and the target area low level met message (MET-TALL). The last component, the Met Message Dissemination Report, compares new MET-CMs with those previously disseminated to fire support units and determines whether they have changed enough to significantly affect artillery accuracy. If they have not, it recommends against dissemination of the new messages to avoid unnecessary communications traffic.

Contents

Figures

Tables

Executive Summary

This report contains basic information on the theoretical and practical meteorological (met) principles employed in the Computer-Assisted Artillery Meteorology (CAAM) system using the Battlescale Forecast Model (BFM). In CAAM (BFM) several types of met inputs are assimilated and processed in order to produce artillery met messages on the battlefield. Central to this system is the use of a mesoscale atmospheric prediction model (the BFM). This report's introduction gives a history of the program and an overview of the design of CAAM. The model domain is described in terms of an Area of Operations (AOP) in addition to the data required to operate the model. The three-dimensional objective analysis (3DOBJ) used for model initialization is described for two modes: with and without the input from a large-scale forecast model. The initialization and nudging methods used in the BFM are also described fairly extensively; however, in view of already existing documentation, the forecast model itself is only briefly described here. The output of CAAM consists of two kinds of artillery met messages; these are derived from both the objective analysis and the BFM results. Finally, future improvements and developments are mentioned.

1. Introduction

1.1 Purpose and Overview

This report presents basic information on the theoretical and practical principles employed in the Computer-Assisted Artillery Meteorology (CAAM) Battlescale Forecast Model (BFM) system (referred to as the CAAM (BFM) system, or more simply as CAAM). CAAM assimilates a variety of meteorological (met) inputs in the battlefield, processes and forecasts these data through a mesoscale forecast model (the BFM), and outputs improved artillery met messages tailored for specified gun and target locations.

This report primarily addresses the met components of CAAM. Sections 2 through 5 discuss the issues of model domain, objective analyses, mesoscale modeling, and generation of MET-CMs. Section 6 reviews the previous sections and touches on future developments and recommendations. The remainder of this introduction gives a brief history of the CAAM project and its internal organization.

1.2 Background

The U. S. Army Field Artillery has relied on balloon-borne radiosonde soundings for met support since shortly after World War II. The delivery of the AN/TMQ-31 Meteorological Data System (MDS) to Army Field Artillery Units (last deliveries in 1984) improved the mobility of met sections and added the capability of data acquisition through the use of navigation-aid systems such as LORAN or International OMEGA. Although wind speed and direction estimates were improved, the principle of balloon-borne soundings from no more than three locations in the friendly area of a division zone of responsibility had not changed from the traditional way of using the met data. This limitation can result in both temporal and spatial "staleness" degrading the information in the met messages.

In the early 1990's, it was recognized that more advanced met approaches could be used to improve the met messages on which the Field Artillery relied for aiming adjustments. The Army Research Laboratory (ARL) Artillery Meteorology Branch, with assistance from other Army agencies, began a two-phase research

and development effort for improving artillery meteorology with computer assistance (i.e., CAAM). [1] Phase One of CAAM was based on the Time-Space Weighted model (TSW). [2] This technique combines available met messages on the battlefield to interpolate tailored "best" met messages for users based on the distances and ages of the input messages from the location and time of application. CAAM (TSW) is now in the process of being integrated into the AN/TMQ-41 Meteorological Measuring Set, the modern replacement for the MDS.

Phase Two of CAAM began in 1993 and is now referred to as CAAM (BFM). This CAAM satisfied its Advanced Technology Demonstration in September 1994, and in May 1995 supported an artillery live-fire exercise at the Marine Corps Air Ground Combat Center, Twenty-nine Palms, CA. The results of this exercise and a post-analysis are documented. [3] CAAM (BFM) is far more complex than CAAM (TSW) in that it uses numerous and diverse met inputs, and a more sophisticated analysis process which includes a mesoscale forecast model (the BFM). This advanced processing allows it to produce improved met messages not only for conventional gun/target distances, but also for distant target areas. The improved characterization of target area meteorology is important in estimating when and where to employ submunitions that are deployed above the target, and are therefore affected by local target, low level conditions.

1.3 Overall System Design

CAAM (BFM) has undergone a series of modifications and improvements since its original design, and is now in version 4. [4] The current major components of the CAAM system, the top-level user interface options, and the types of input met data are shown in figure 1. These data are presented in detail in section 2 of this report. In the discussion that follows, refer to figure 1.

The CAAM software is written primarily in Ada with some FORTRAN components (including the BFM itself). There are several separate programs which are all integrated by the main program's interactive Executive component. The user's main function is to initialize the Area of Operations (AOP) by entering the area to be modeled and the gun/target locations (for which met messages will be generated). The AOP Initialization component prepares the model-domain related files that are required for modeling (see section 2). The remaining

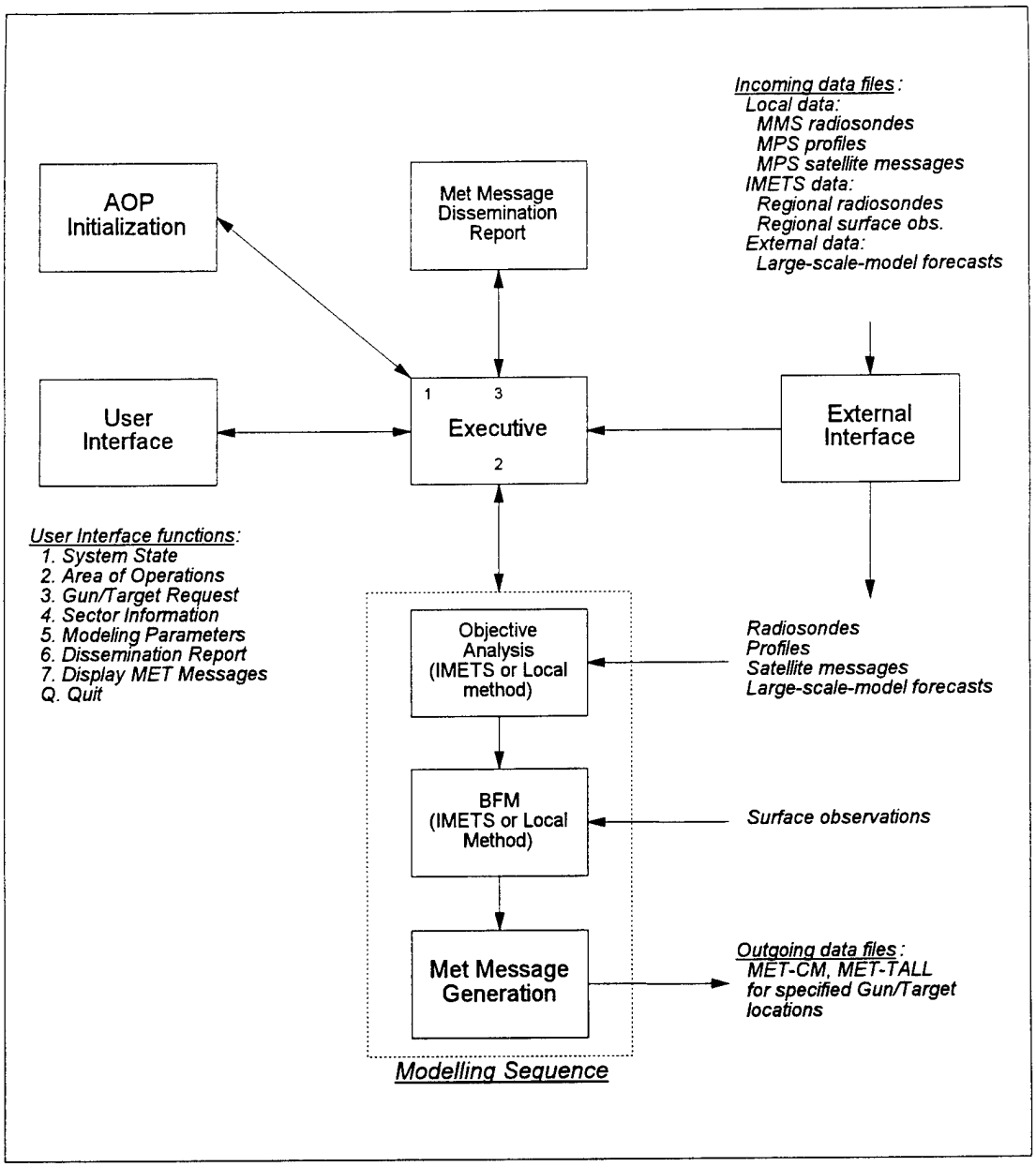

Figure 1. CAAM (BFM) organization and software components.

functions are highly automated, but they can be more finely controlled for research and analysis purposes.

Six types of met input files are received and managed by the External Interface component. Once sufficient data are present, and the AOP has been initialized, the modeling sequence can begin. This sequence has three components which are executed in series:

- objective analysis (two possible methods, see section 3),
- BFM (two possible methods, see section 4), and
- met message generation (see section 5).

When the sequence is completed, two types of met messages will have been generated: the computer met message (MET-CM) and the target area low level met message (MET-TALL). The last component of the sequence, the Met Message Dissemination Report, compares new met messages with those previously disseminated to fire support units and determines whether they have changed enough to significantly affect artillery accuracy. If they have not changed sufficiently, the report recommends against dissemination of the new messages to avoid unnecessary communications traffic. This component uses firing table data and a rule-base to make its decisions, but a further description is beyond the scope of this report.

2. CAAM Model Domain

2.1 AOP

The CAAM AOP establishes the geographic area of the modeling domain. This domain is then defined in terms of three-dimensional grids; the initial grids are those produced by the objective analyses of winds, temperature, and moisture. These grids, in turn, are used to initialize and provide time-dependent lateral boundary conditions for the forecast model (the BFM), whose output is also gridded.

The "typical" dimensions of the CAAM AOP are those of the original CAAM contractual requirements: 220 km long (in the downrange direction) and 60 km wide. An example of such an AOP is shown in figure 2. The geographic positioning of the AOP is determined when the user enters the center of the Forward Line of Own Troops (FLOT) and the azimuth of the downrange direction (i.e., in the threat direction). The FLOT is assumed to be 20 km from the friendly end of the AOP.

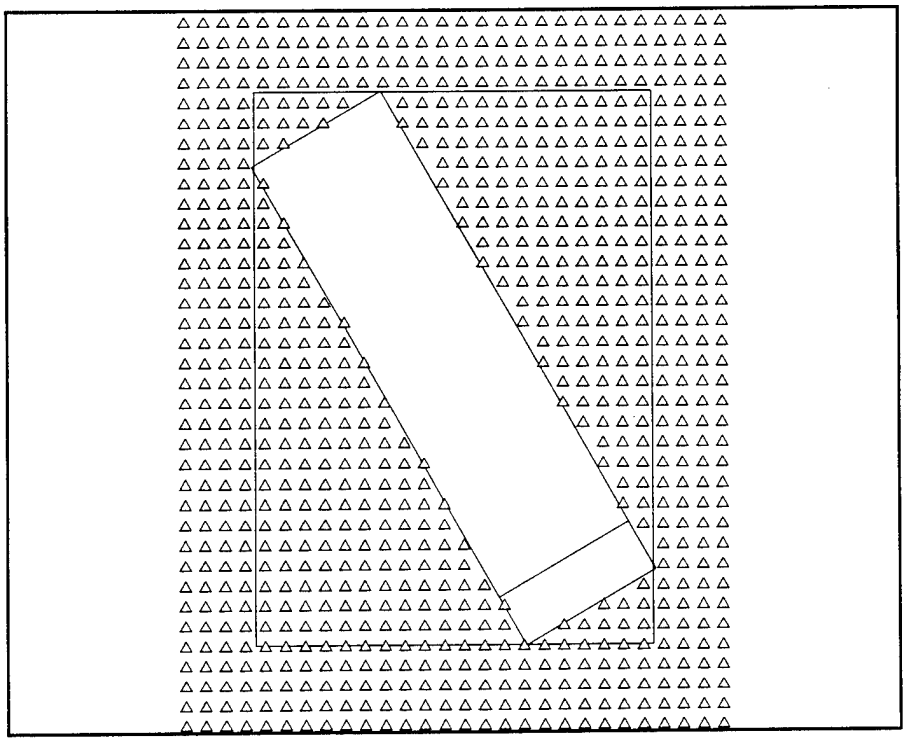

Figure 2. CAAM horizontal grid for angled AOP with minimum bounding rectangle.

In figure 2, the downrange azimuth is 330°. The horizontal grid points at a uniform spacing of 8 km are also shown. The actual model domain is the minimum bounding rectangle around the AOP. The smallest CAAM model domains occur for AOPs that are oriented north-south or east-west, in which cases the minimum bounding rectangles are the same as the AOPs.

In practice, the CAAM AOP is not limited to the typical case. It may be any rectangular area up to 500 km on a side. In larger AOPs, the horizontal grid spacing should be increased to reduce the total number of points (and computation time). Smaller AOPs should have correspondingly smaller grid spacings.

In the case of CAAM, rapid production of forecasts is a necessity. Having a small AOP is attractive because the forecast model can be run on a desktop PC in as little as 15 min, an impossibility with a larger domain. Nonetheless, it should be noted that the typical CAAM AOP domain (about 200 km on a side) is somewhat small for making lengthy forecasts because inflow through the lateral boundaries can rapidly dominate the conditions in the forecast domain. For example, a wind of 50 m/s flowing across the AOP implies that conditions at the inflow lateral boundary will impact interior points in the domain at the inward rate of 180 km/hr. Conditions in the forecast domain may thereafter be dominated by the inflow. Although it should always be better to have a larger domain in order to postpone as long as possible the effect of the lateral boundaries, it is not always possible to do so because of computational constraints. This effect can be reduced significantly by having a larger scale model frequently supply the information for both the large-scale flow and inflow lateral boundary condition; this is the approach used in the BFM.

2.2 Horizontal Grids and Vertical Levels

As discussed above, in any AOP the horizontal grid spacings are constant in both directions, and the model domain is limited to 500 km on a side. Thus, the typical AOP of 220 x 60 km with 8-km grid spacing results in a 35 x 15 grid. This AOP area is actually 272 x 112 km in extent because extra grid points are added around the initial 220 x 60 km area to serve as a buffer around the central area where the data are most important. These extra grid points are shown in figure 2 as the points surrounding the AOP's minimum bounding rectangle.

The number and spacing of vertical levels is more complex and is discussed more fully in section 3.1. In the objective analyses there are 55 flat levels at predetermined heights extending to 30 km above the minimum surface elevation. These 55 levels provide 1-km resolution at higher levels and finer resolution closer to the ground. The BFM models in a terrain-following coordinate system of 32 levels. The objective analysis on the 55 flat levels is linearly interpolated to these 32 levels for BFM initialization and boundary conditions, and the BFM outputs its grids at these levels.

2.3 Terrain Elevation Data

As part of the initialization of files for the model domain, two terrain elevation data files are generated. The elevation data are read from Defense Mapping Agency's Digital Terrain Elevation Data (DTED) CD-ROMs. These data are Level One, which have a horizontal resolution of 3 arc-seconds, or about 92 m in the north-south direction (less in the east-west direction, depending on latitude).

The first data file generated is that required by the BFM, and it is at the same horizontal resolution and coverage as the BFM grid. This file is required because the BFM operates in a terrain-following coordinate system (see section 4).

The second data file is referred to in CAAM as the "high-resolution" terrain file. This file also covers the BFM grid, but the horizontal resolution is 500 m. It is used to interpolate the met datum planes (surface elevations) of met messages generated for gun/target pairs.

2.4 Input Met Data

Table 1 shows the types of met files that are input and processed by CAAM as well as the sources and expected arrival frequencies of these files. The current Mobile Profiler System (MPS) source is a prototype.

Table 1. Types of met data input by CAAM

Type	Source	Expected Frequency
Local radiosondes	MMS	1/hr
Local profiles	MPS	4/hr
Satellite profiles	MPS	4/day
Regional radiosonde sets	IMETS	2/day
Regional surface observations	IMETS	1/hr
Larger scale model (NOGAPS) forecast sets	IMETS	2/day

MMS: Meteorological Measuring Set

MPS: Mobile Profiler System

IMETS: Integrated Meteorological System

3. Three-Dimensional Objective Analysis

Numerical weather forecast models depend critically on the establishment of both the initial conditions of all variables on the BFM calculation grid and the lateral boundary conditions of the model domain. This is accomplished by performing a three-dimensional objective analysis (3DOBJ) of the available data. The best analysis would include the input of a larger scale forecast model, but it is possible to make a 3DOBJ without this guidance. Radiosonde or other available upper-air data, produced as a part of twice-daily World Meteorological Organization releases (12Z and 00Z) by national met services or as special support for artillery or other Army operations, are required to produce this 3DOBJ. Since the CAAM system may receive different types of data (section 2), the objective analysis is complex in order to handle the multiplicity of possible data situations.

The current model used for large-scale forecast data is the Naval Operational Global Prediction System (NOGAPS), produced at the Fleet Numerical Oceanographic Center. There are two main objective analysis procedures: with and without NOGAPS data. With NOGAPS data, the objective analysis procedure is similar to that employed by the Integrated Meteorological System (IMETS) version of the BFM, where both NOGAPS and radiosonde data are used to produce a 3DOBJ of the met fields in the AOP at initial- and final-run times. The initial field is a composite of the upper-air analysis from the rawinsonde (radio wind sounding) observations (RAOBs) and the analysis from NOGAPS. Without NOGAPS data, objective analysis procedures originated by Caracena are used to produce an initial-time 3DOBJ. [5]

In either analysis procedure, upper-air sounding data are required, and the following quality-control checks are performed on the data prior to usage:

- All geopotential values in the 500 to 880 mb pressure range that depart more than 15 percent from a standard atmosphere are flagged.

- All geopotential values below 880 mb that depart more than 20 percent from a standard atmosphere are flagged.

- Any small values of pressure gradient (< 0.02 mb/m) found near the surface are flagged.

- Large inversions are eliminated except at the surface, where an inversion as large as 400 °C/km is permitted.

- Extreme superadiabatic layers with lapse rate exceeding -22 °C/km are eliminated except near the surface, where lapse rates less than autoconvective are allowed.

- After gross error checks, height and temperature fields are checked using the hypsometric relationship.

- Vertical wind shears in excess of 150 kn/km are eliminated.

3.1 Vertical Coordinates

Either analysis procedure produces two sets of initial fields, both at the BFM's horizontal resolution. The first set is at 55 flat levels, starting at the height of the lowest terrain point and extending vertically to the extent of the available data, up to 30 km. This set is used if the BFM run is not desired or to fill in above the top of the BFM for output met messages. The second set is done at the model pseudo-terrain-following vertical levels. These data fields are used to initialize the BFM and to specify the time-dependent lateral boundary conditions. In the CAAM (BFM), both the analysis and forecast domains are coincident.

The pseudo-terrain-following coordinate exactly follows the terrain at the surface of the Earth and is a flat z-level at the top. The physical height of the pseudo-terrain-following vertical coordinate, z*, varies with each gridpoint terrain height and the defined level z. The value z* is defined as:

$$z^* = \overline{H}\,\frac{z - z_g}{H - z_g} \qquad (1)$$

where z is the vertical coordinate in a cartesian system, z_g is the ground elevation, and H is a specified model top above ground level in the z* coordinate system.

H is defined from $H = \overline{H} + z_{gmax}$, where z_{gmax} is the maximum surface elevation in the AOP. For example, for a model set up to run with an AOP over White Sands Missile Range (WSMR) with a z_{gmax} of 3035 m and a vertical extent of 12000 m (model top = 3035 + 8965 = 12000 m/asl), the met forecast parameters are defined at 32 levels. At the gridpoints with the maximum terrain elevation, z_{gmax}, each vertical level is located at a cartesian height, z, above ground level exactly equal to the height specified by z*; that is, at gridpoint (I_{zgmax}, J_{zgmax}), z = z* for each level. These levels would be lower and physically stretched at other gridpoints. The levels are given in table 2:

Table 2. Example of vertical coordinates used in CAAM

Level	Z height (z*) (m)	Level	Z height (z*) (m)	Level	Z height (z*) (m)	Level	Z height (z*) (m)
1	0.0	9	226.0	17	1810.4	25	4947.0
2	4.0	10	339.2	18	2117.6	26	5448.3
3	8.0	11	476.6	19	2449.0	27	5973.7
4	12.0	12	638.3	20	2804.7	28	6523.5
5	16.0	13	824.2	21	3184.7	29	7097.5
6	32.1	14	1034.3	22	3588.9	30	7695.7
7	72.5	15	1268.8	23	4017.3	31	8318.2
8	137.1	16	1527.4	24	4470.1	32	8965.0

These are the model levels (z*) at which the prognostic variables are computed.

3.2 Three-Dimensional Objective Analysis Procedure with NOGAPS Data

Time-dependent lateral boundary values provided by a large-scale forecast model such as NOGAPS should be used by the BFM in generating its forecast. These fields are obtained through a complex process that begins with linear time interpolation of the large-scale forecast fields. There are two requisites for using this process: valid large-scale model output must be available, and there must be at least one acceptable radiosonde sounding in the time period. CAAM has available (through IMETS) the large scale forecast model fields of the NOGAPS. Currently, NOGAPS data consists of 12-, 24-, and 36-h forecast fields. If the

BFM start-of-run falls between these forecast times, the initial fields are obtained through linear interpolation of the beginning and ending NOGAPS forecasts of the appropriate 12-h period. A later section will describe how upper-air radiosonde data are used to modify the NOGAPS fields by the compositing process.

When NOGAPS data are available, the 3DOBJ model first selects the proper times for the output of the objective analyses (at the run start and end). Then, the NOGAPS data are acquired, quality checked, and analyzed to the NOGAPS pressure levels. These analyses are then interpolated to the 55 flat levels used to analyze the radiosonde data. Then, over a time loop, at each time where there are radiosonde reports, these data are merged with the existing analysis interpolated to the time of the data. The difference between the time-interpolated NOGAPS data and the merged analysis at each grid point and time is saved in order to form an average deviation at each grid point. This average is applied to the time-interpolated NOGAPS analyses valid at the time of the start and the end of the model run. The 55-level analysis is output for use when the BFM cannot run or for filling in the top of met messages above the highest BFM level. These analyses are then interpolated to the 32 pseudo-terrain-following levels.

3.2.1 Analysis of the NOGAPS Data

The NOGAPS model output fields are on the Air Force Global Weather Central (AFGWC) whole-mesh grid (horizontal spacing of 381 km) at six constant pressure levels (200, 300, 500, 700, 850, and 1000 mb). The model output variables are:

- geopotential height, Φ (m);
- temperature, T (°K);
- dewpoint depression, T_D (°K); and
- horizontal wind components, U and V (m/s) transformed onto the AFGWC grid.

These fields are converted to the following variables on flat levels (and then later at the terrain-following vertical levels at each grid point):

- potential temperature (°K);
- water vapor mixing ratio (g/kg);
- easterly-directed wind, u, (m/sec);
- northerly-directed wind, v, (m/sec); and
- surface pressure distribution (mb).

NOGAPS values for u, v, T, T_D, and Φ on pressure levels are horizontally interpolated to the CAAM grid points using a Barnes-type weighting to obtain a "first guess" which is then corrected according to the differences between the first-guess field and NOGAPS values at NOGAPS grid points. For any variable ψ, the first-guess values for any model grid point (i,j) are calculated from:

$$\psi(i,j) = \frac{\Sigma_N \psi_N \exp(-\frac{(r_{ij,N})^2}{4k})}{\Sigma_N \exp(-\frac{(r_{ij,N})^2}{4k})} \qquad (2)$$

The exponential weighting follows from Barnes in which $r_{ij,N}$ is the normalized distance between a grid point (i,j) and the N^{th} NOGAPS point, and k is an empirical parameter that determines the shape of the weighting function. [6] The value ψ_N represents the observed value at the N^{th} NOGAPS point. Applying equation (2) to the AOP grid yields fields of first-guess values for the five met variables listed above. Since few or no NOGAPS grid points lie within any CAAM AOP, equation (2) is also applied to NOGAPS points even if they lie outside the AOP but are within an approximately 1600 km x 1600 km area which includes the AOP.

Naturally, the agreement at this stage between the first-guess field and the observations is not optimal and may be improved by considering the average difference, Δ, between the first-guess field and the NOGAPS at the NOGAPS points:

$$\Delta\ (i,j)\ =\ \frac{\Sigma_N\ \Delta_N\ \exp(-\ \frac{(r_{ij,N})^2}{4\gamma})}{\Sigma_N\ \exp(-\ \frac{(r_{ij,N})^2}{4\gamma})} \tag{3}$$

where γ is an empirical weight factor (0.2) and Δ_N is the difference for the Nth NOGAPS point. The average difference, $\Delta_{(i,j)}$, is distributed to the AOP grid points, making the final analysis value of ψ at (i,j):

$$\psi_f(i,j)\ =\ \psi(i,j)\ +\ \Delta(i,j) \tag{4}$$

In order to obtain values of ψ on the z* levels, the ψ_f values in equation (4) are linearly interpolated from the constant pressure levels as a function of height or:

$$\psi(z^*)\ =\ \psi_k\ +\ \frac{\psi_{k+1}\ -\ \psi_k}{\phi_{k+1}\ -\ \phi_k}\ (z_{st}\ -\ \phi_k) \tag{5}$$

where z_{st} denotes the height above sea level of z* calculated from equation (1) as:

$$z_{st}\ =\ z_g\ +\ z^*\ \frac{(\bar{H}\ +\ z_{gmax}\ -\ z_g)}{\bar{H}} \tag{6}$$

In complex terrain, because of the altitude variation of the underlying terrain, the surface pressure field can vary considerably. When the surface height geopotential lies between the geopotentials of two adjoining pressure surfaces (i.e. $\phi_2 > z_g > \phi_1$ and $z_g - \phi_1 \leq \phi_2 - z_g$) the following method is used. The hypsometric equation for the surface pressure is:

$$P_{sfc} = P_1 \exp\left[\frac{g}{R_d \bar{T}} (z_g - \phi_1)\right] \quad (7)$$

where

$$\bar{T} = T_1 + \frac{T_2 - T_1}{\phi_2 - \phi_1} (\bar{Z} - \phi_1) \quad (8)$$

and

$$\bar{Z} = \frac{(z_g + \phi_1)}{2} \quad (9)$$

If $z_g - \phi_1 \geq \phi_2 - z_g$, then

$$P_{sfc} = P_2 \exp\left[\frac{g}{R_d \bar{T}} (\phi_2 - z_g)\right] \quad (10)$$

where

$$\bar{T} = T_1 + \frac{T_2 - T_1}{Z_2 - Z_1} (\bar{Z} - Z_1) \quad (11)$$

and

$$\bar{Z} = \frac{(z_g + \phi_2)}{2} \quad (12)$$

By this method, fields of potential temperature, dewpoint temperature, and the horizontal wind components are analyzed on constant pressure surfaces as received from the NOGAPS. Then the resulting values are linearly interpolated in the vertical to 55 vertical layers. This procedure is done at all the 12-h NOGAPS forecast times required to make the CAAM forecast. For example, a

4-h CAAM forecast initialized at 16Z would utilize analyses based on 12Z and 24Z NOGAPS data for these purposes, while a 6-h CAAM forecast initialized at 20Z would require, in addition to these, an analysis of the following day's 12Z NOGAPS data. This step yields a first-guess analysis of these fields.

3.2.2 Compositing of Upper-Air and NOGAPS Data

With the NOGAPS data analyzed, a time loop is entered. Since a CAAM forecast may begin at times well removed from the regular upper-air synoptic data collection times of 00Z and 12Z (for example, 06Z or 18Z), it is important to incorporate observations made at asynoptic times into the analysis procedure. At each time upper-air data are available, a compositing technique is used to produce a 3DOBJ. This technique merges the time-interpolated NOGAPS field valid at the time of the available upper-air sounding with those upper-air soundings. The upper-air sounding data are vertically interpolated to the same 55 vertical levels used for the first-guess field. At each level, the average error, $\bar{d}$, between the first-guess field, $\Psi_{G,N}$, and the upper-air observations, $\Psi_{U,N}$, is calculated at the upper-air observation positions as:

$$\bar{d} = \frac{\sum_{N=1}^{N_{obs}} (\Psi_{G,N} - \Psi_{U,N})}{N} \tag{13}$$

where $\Psi_{G,N}$ is obtained from the objective analysis of the NOGAPS data at the N^{th} upper-air observation point, $\Psi_{U,N}$ is from the corresponding upper-air data at that point, and N_{obs} is the number of observations. The average error, $\bar{d}$, is added to the entire first-guess field:

$$\Psi^*_G(i,j) = \Psi_G(i,j) + \bar{d} \tag{14}$$

thereby removing the mean error. This still leaves a local error:

$$d^*_N = \Psi_{U,N} - \Psi^*_{G,N} \tag{15}$$

whose mean, $\bar{d}^*$, is zero. The local error can be reduced by objectively analyzing d^* using a $1/r^2$ weighting function as:

$$\Psi^{**}{}_{G}(i,j) = \Psi^{*}{}_{G}(i,j) + \frac{\sum_{N=1}^{N_{obs}} \frac{d^{*}{}_{N}}{r^{2}{}_{ij,N}}}{\sum_{N=1}^{N_{obs}} \frac{1}{r^{2}{}_{ij,N}}} \qquad (16)$$

In the CAAM (BFM) implementation of this technique, the important outcome of this step is not to get a "best" analysis at each time, but rather to determine the difference between the time-interpolated NOGAPS data and the upper-air soundings at each time. These differences are saved to provide an average difference over all times at which there are data available. This process is valid only up to the top of the NOGAPS. Above this level, additional techniques are required.

3.2.3 Objective Analysis Above the NOGAPS Top

Currently, information from the NOGAPS is only available up to and including the 200 mb surface, which is at a height of about 12 km. However, conceivable artillery needs require information up to 30 km. To partly achieve this requirement, the objective analysis procedure from 12 km to as high as 30 km relies solely on available upper-air RAOBS. The first time in which data are available above the top of the existing analysis, they are analyzed. At each subsequent time in which data are available, they are composited to the previous analysis. With time, the prognostic fields below 12 km evolve, while those above 12 km receive no forecast application. Consequently, they will increasingly disagree with those below. Therefore, a blended merging of both is done above the NOGAPS vertical domain (i.e., between 12 and 30 km).

The blended merging consists of a hyperbolic tangent weighting in which, at 12 km, the NOGAPS-based prognostic fields are weighted as 1 and the purely objective analysis fields as 0. At 20 km, the reverse is true. Equal weighting occurs at 16 km. As the NOGAPS-based fields evolve, the difference between them and their initial condition receives the blended weighting as described above. In other words, the fields above 12 km evolve according to the developing

difference at 12 km, with this weighting decreasing to 0 at 20 km where the initial conditions are maintained.

3.2.4 Analyses at Start and End Times

The final analyses are produced after completion of the time-loop compositing of the available upper-air data to the time-interpolated NOGAPS fields. If the desired initial time of the CAAM run is between 12Z and 00Z, then linear time interpolation is performed using the NOGAPS-based analyses at the two above times to establish the initial and final conditions of the model forecast. For example, with a 15Z initial time and a 4-h forecast, the two analyses at the encompassing NOGAPS endpoints (12Z and 00Z) are used in making a linear interpolation to both the start and finish time of the model forecast period. With just upper-air observations available at 12Z, the corrections at each grid point obtained by compositing to the 12Z NOGAPS field are added to both the start (15Z) and finish (19Z) time-interpolated fields. If there is also asynoptic information such as local upper-air observations at 13Z and 14Z (as shown in figure 3), this information is composited to the linearly interpolated fields for those times, and the average differences are computed. This is done by combining the differences from compositing the 13Z and 14Z data along with the differences from the 12Z upper-air compositing. The resulting averages are added to both the start and finish fields.

If the model start and finish times fall into different 12-h NOGAPS periods, an additional technique is required. For example, we modify our example above to have a start time of 19Z and specify a 6-h forecast with a finish time of 01Z. Now the finish time falls into the following 12-h NOGAPS time period. While the model start conditions can be obtained as in the previous example, the model finish time conditions must be obtained from time interpolation between the 00Z analysis (24-h NOGAPS forecast) discussed above and the succeeding 12Z analysis (36-h NOGAPS forecast). As before, the average differences obtained from compositing all the upper-air observations are added to the time-interpolated model end time field at 01Z.

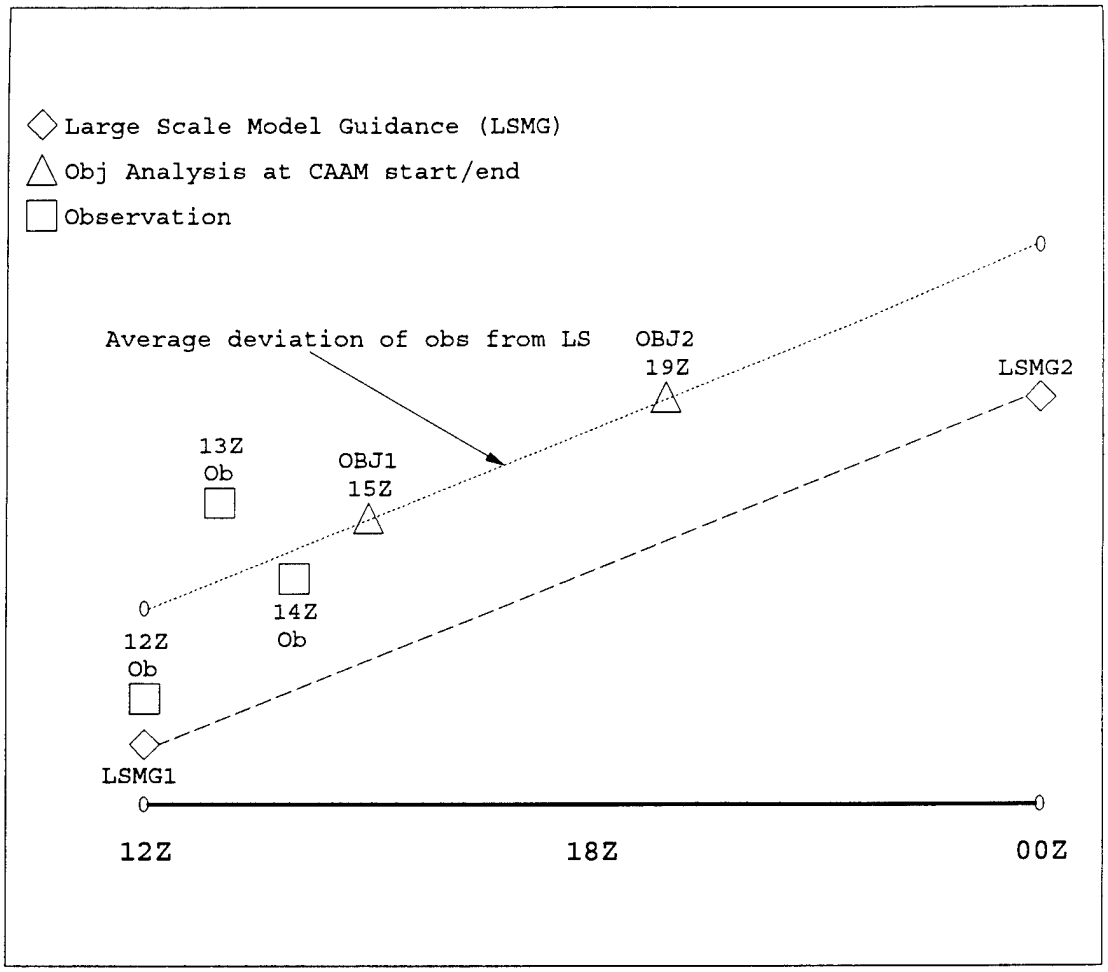

Figure 3. Start and finish conditions for a 4-h forecast beginning at 15Z.

3.3 Three-Dimensional Objective Analysis Procedure without NOGAPS Data

Without NOGAPS guidance, only observed upper-air data is available. In this case, the analytic approximation, or multipass, approach originated by Caracena is used to produce a three-dimensional analysis. [5] In order to extract the maximum information from such limited data, observations that are several hours old may be utilized. There are two means of incorporating older data: time-space weighting and time trending. A time-space weighting framework is applied to spatially separated sources of data which may also be time separated. A second method of incorporating older data consists of using two or more observations in time at the same location, allowing a time trend to be established. In this section,

we will first discuss the time trending and time-space weighting of data used in Caracena's multipass procedure, before describing the procedure itself.

3.3.1 *Time Trending Data*

Time trending consists of a linear least squares fit in time to a series of observations at a single location. This fit may be extrapolated to either the model start time, if it is within 2h from the latest observation, or up to a maximum of 2h, if necessary, to obtain more recent estimates of the data values. This technique yields new observation data that are permitted in the analysis under the time-space weighted framework (see below) with the time-trended time. For example, given a model start time of 20Z, an observation at one location at 19Z, and observations at 13Z and 16Z at another location, the 13Z and 16Z observations are time trended to 18Z. The observation at 19Z at the first location and the time-trended observation valid at 18Z at the second location are time-space weighted in the analysis.

3.3.2 *Time-Space Weighting of Data*

In time-space weighting, the time separation between the time of an observation and the time of its application is converted into an effective spatial separation. In CAAM, 1 h of time separation is considered equivalent to 30 km in spatial separation. The 30-km value represents a compromise between reported variability equivalences from as large as 46 km = 1 h to as small as 10 km = 1 h over homogeneous terrain. [2] For complex terrain, such as mountainous and coastal regions, even smaller distances should be used. The purpose of time-space weighting is to maximize utilization of scarce data, but in a manner reflective of its fidelity in portraying the situation at the time of model initialization. Time-space weighting and conversions between time and space are discussed more extensively by Blanco. [2]

3.3.3 *Analytic Approximation*

Under Caracena's analytic approximation, or multipass, approach, the objective analysis by weighted sums (such as a Gaussian weighting) is generalized by analytic functions. [7] Although Caracena intended to utilize this method at

discrete points as opposed to a regular array of grid points, it is also useful for the latter application. The analytic function is used to compute weights contained in the weighted sums. The weighting function is isotropic, homogeneous, and dependent only on the four-dimensional (space and time) separation between the observation location and the point at which it is evaluated. [8] The derivatives of weighted sums generate derivatives of the analytic approximations which are, in turn, weighted sums. The resulting expressions are greatly simplified when a Gaussian function is used for the weight, as is the case here, because the analytic approximation of a field and its derivatives contain the same set of weights.

The analytic approximating function <F>(r) is written as the sum of products of observations f_k and corresponding weight functions $w_k(L,r)$:

$$<F>(r) = \sum_{k=1}^{S} f_k w_k(L,r) \tag{17}$$

where the weight functions are:

$$w_k(L,r) = \frac{\exp[\frac{-|r - r_k|^2}{L^2}]}{\sum_{j=1}^{S} \exp[\frac{-|r - r_j|^2}{L^2}]} \tag{18}$$

In equations (17) and (18), S is the number of observations, and L is a scale parameter that controls the width of the weighting function. [5] However, in this project, equation (18) had to be modified because of the need to use time-space weighting. Due to the additional exponential decrease of the weight brought about by time weighting, the values of $\exp(-R^2)$ approached zero too rapidly. Therefore, exp(-R) was used in CAAM to accommodate the time-space weighting, and the equation for weights became:

$$w_k(L,r) = \frac{\exp[\frac{-|r - r_k|}{L^2}]}{\sum_{j=1}^{S} \exp[\frac{-|r - r_j|}{L^2}]} \qquad (19)$$

Note that the r used in equation (19) includes both the spatial distance between the observation and analysis points and the effective spatial distance as converted from the time difference between the observation and the model initialization time. At a distance L from an observation point, the weighting is 1/e of its peak value. As constructed, the weighting functions above are normalized so their sum is 1 at any location r. Derivatives of the analytic approximating function are obtained by partial differentiation of it, with the observations, f_k, treated as constant. Because of use of the Gaussian weighting scheme, the derivatives, and hence gradients, are fairly simple.

When performing an analysis, if only one pass is done, there is a noticeable loss of amplitude when an appropriate smoothing is used; if not, a serious distortion is produced due to spurious short-wavelength noise. These responses depend on the smoothing length used. By performing multiple passes on the observations with appropriate smoothing, the response of the analysis can be improved. This is accomplished by computing the differences between the observations and the corresponding value of the observed field and then objectively analyzing this onto the analysis. This successive-correction approach appears to acceptably converge within just a few passes depending on the number of available observations (the method is possibly less efficient for small numbers of observations). For each pass, the same smoothing length is used. Under the analytic approximation, the successive corrections can be accomplished through compact matrix manipulation, owing to the recursive nature of the Gaussian weighting functions, as long as the same smoothing length scale is used.

The first-pass field can be expressed as:

$$\langle F \rangle^{(1)} = \boldsymbol{w}^T(\boldsymbol{r})\boldsymbol{f} \qquad (20)$$

Since $<F>^{(1)}$ can be evaluated anywhere in the analysis domain, it can be evaluated at an observation point r_l. The difference between it and the observation value at that point is:

$$\delta^{(1)}f_l = f_l - <F>_{(r_l)}^{(1)} \tag{21}$$

The differences represented by equation (21) for all the observation points are objectively analyzed and added to the previous analysis to give:

$$<F>^{(2)} = <F>^{(1)} + <\delta F>^{(1)} \tag{22}$$

in which the objective analysis of the difference field is:

$$<\delta F>^{(1)} = \boldsymbol{w}^T(\boldsymbol{r})\delta^{(1)}\boldsymbol{f} \tag{23}$$

By continuing with a series of n corrections, the n^{th} correction in terms of the $n\text{-}1^{st}$ pass is:

$$<F>^{(n)} = <F>^{(n-1)} + <\delta F>^{(n-1)} \tag{24}$$

where

$$<\delta F>^{(n-1)} = \boldsymbol{w}^T(\boldsymbol{r})\delta^{(n-1)}\boldsymbol{f} \tag{25}$$

and

$$\delta^{(n-1)}f_j = f_j - <F>_j^{(n-1)} \tag{26}$$

In practice, there are a number of ways of implementing the multipass scheme. The most familiar might be to accumulate the corrected fields on regular grids and update them on each pass through the grid. The method used in CAAM, termed the matrix method by Caracena, uses a matrix of weights between observation sites to produce an effective n-pass array that is used in a single pass. [5] This

latter method begins with a matrix of weights between stations:

$$W_{ij} = w_j (r_i). \tag{27}$$

Then, combining equations (24), (25), and (26) with equation (27) yields the general expression for an effective n-pass analytic approximation:

$$\langle F \rangle^n = w^T(r) W^{-1} [I - (I - W)^n] f \tag{28}$$

where I is the identity matrix of dimension equal to the number of observations. As mentioned above, Caracena completed a number of tests of this scheme and concluded that n = 4 produced good results, with no distinct improvement noted for n greater than 4. Despite the success of this scheme, it cannot be expected to make up for a paucity of observations. [1] A related question is the distribution of the observations with respect to the analysis domain. Several observations clustered near one spot in the domain will also cause analysis problems.

4. Mesoscale Forecast Model

The Higher Order Turbulence Model of Atmospheric Circulation (HOTMAC), developed by Yamada and adapted by Henmi and Dumais, is employed in CAAM. [9] [10] This model is currently referred to as the BFM. This section will discuss the techniques of initialization, nudging to observations, nudging to target winds, surface data assimilation, and forecast equation solving. In the descriptions that follow, the differences between the operation of the BFM with and without the NOGAPS guidance are also highlighted.

4.1 Initialization

In initializing the BFM, the θ_v field obtained from the 3DOBJ is used and is called the base state, or $<\theta_v>$, field. At model initialization, the smaller of two values, either the reference atmosphere wind at the top of the assumed boundary layer (UMAX0, m/s) or (0.4/k) log[(z*+0.1)/0.1], is used for the wind speed.

In order to introduce the real wind fields in a dynamically adjusted fashion, a 3-h model spin-up time going from the initial winds to those obtained from the objective analysis is performed. The dynamic adjustment from spin-up to objective analysis is accomplished by the nudging method described below. During the spin-up, model surface temperatures are also nudged to surface observations valid at the initial model time. This will also be described below.

4.2 Nudging Method

In order to assimilate the synoptic changes available from the NOGAPS boundary-condition three-dimensional analyses, nudging terms are added to the right-hand sides of the predictive equations for the horizontal wind components, for potential temperature, and for the water vapor mixing ratio. For horizontal winds, the nudging takes the form of the following two equations:

$$\frac{\partial U}{\partial t} = F_1 + C_n(U_t - U) \tag{29}$$

and

$$\frac{\partial V}{\partial t} = F_2 + C_n(V_t - V) \tag{30}$$

where C_n is the nudging coefficient, and U_t and V_t are the target wind components in the x and y directions, respectively. The target winds are discussed further below. F_1 and F_2 are the forcings on the right-hand side of the equations of motion for the u and v wind components, respectively.

The predictive equations for potential temperature deviation and mixing ratio are also subjected to nudging. For potential temperature deviation, the nudging takes the form:

$$\frac{\partial \delta\theta}{\partial t} = F_3 + C_n(\delta\theta_{obs} - \delta\theta) \tag{31}$$

while the nudging for the mixing ratio is:

$$\frac{\partial Q_v}{\partial t} = F_4 + C_n(Q_{v,obs} - Q_v) \tag{32}$$

where $\delta\theta$ is the potential temperature deviation between the model, θ_v, and the base state, $\langle\theta_v\rangle$. The water vapor mixing ratio is Q_v, and the subscript "obs" denotes the use of observed values based on the objective analysis of the NOGAPS and upper-air data. F_3 and F_4 are the forcing terms of the right-hand sides of the predictive equations for potential temperature deviation and water vapor mixing ratio, respectively. Note that, at the outset, $\delta\theta$ is zero but quickly becomes nonzero during the initialization process as the model dynamically generates a new θ_v field. Based on tests with the model, nudging is not carried down to the surface level. Currently, nudging is applied for vertical layers above $z^* = 150$ m for potential temperature and moisture and above $z^* = 14$ m for the wind components.

When the BFM is run in a "with-NOGAPS" mode, there are initialization fields at the beginning and end of the BFM forecast period. In a with-NOGAPS mode,

the initialization fields at the endpoints are linearly interpolated in time to each hour of the BFM forecast. These hourly values are assimilated into the BFM forecast by the nudging method discussed above.

For the case in which only upper-air and surface (but no NOGAPS) data are available, forecast guidance is obviously not available. Therefore, after the initialization as described above, the nudging continues to the single set of initialization fields. In this case, the magnitudes of the nudging parameters C_n are subjected to an exponential decay, exp(-at), where t is the forecast duration after the initialization time and a is an empirically determined coefficient. The forecast period is expected to be limited to 6 h or less.

4.3 Target Winds

Comparisons between observed and simulated winds have shown that nudging to target winds rather than observed winds produces a better agreement. [9] [10] Target winds are derived as follows. In the absence of friction, the equations of motion for the horizontal wind components are:

$$\frac{\partial U}{\partial t} = f(V - V_g) + C_n(U_t - U) \tag{33}$$

and

$$\frac{\partial V}{\partial t} = -f(U - U_g) + C_n(V_t - V) \tag{34}$$

For $t \to \infty$, the solutions to these equations are:

$$U = \frac{fC_n(V_t - V_g) + f^2U_g + C_n^2U_t}{C_n^2 + f^2} \tag{35}$$

and

$$V = \frac{-fC_n(U_t - U_g) + f^2V_g + C_n^2V_t}{C_n^2 + f^2} \tag{36}$$

Replacing U and V by U_{obs} and V_{obs}, respectively, U_t and V_t are obtained:

$$U_t = U_{obs} - \frac{f}{C_n}(V_{obs} - V_g) \tag{37}$$

and

$$V_t = V_{obs} + \frac{f}{C_n}(U_{obs} - U_g) \tag{38}$$

In equations (37) and (38), U_{obs} and V_{obs} are the x and y components of the observed wind, respectively. With U_{obs} and V_{obs} different from the geostrophic wind components, U_t and V_t are different from the corresponding large-scale wind components. Use of the target winds in the nudging procedure enables the modeled winds to converge to the observations in the absence of friction, as is the case in the free atmosphere. Near the ground, where friction is important, turbulence dominates the nudging terms.

4.4 Surface Data Assimilation

Surface observations are assimilated into the model calculations at grid points in proximity to the observation location. The assimilation is limited to the third and fourth model levels (z*= 8 and 12 m, respectively) and modifies the initial conditions there as:

$$\psi_{new}(i,j) = \psi(i,j) + \frac{\sum_{l=1}^{N} \frac{\psi_l}{r_l^2}}{\sum_{l=1}^{N} \frac{1}{r_l^2}} \tag{39}$$

where ψ_{new} denotes new values of ψ, ψ_l is the observation value of ψ at station l, and r_l is the distance from l to a grid point (i,j). The influence of the nudging is spatially limited by restricting the influence to within a critical distance R as:

$$C_{n,new}(i,j) = C_n + \sum_{l=1}^{N} C_l\left(1 - \frac{r_l^2}{R^2}\right) \qquad for\ r_l < R \qquad (40)$$

and

$$C_{n,new}(i,j) = 0.0 \qquad for\ r_l \geq R \qquad (41)$$

where C_l is an empirical parameter (0.1). The critical distances have been set as 40 km for wind and 20 km for both potential temperature deviation and water vapor mixing ratio. These values were determined empirically and are about three orders of magnitude larger than C_n in order to emphasize the effect of surface data on the model fields.

Assimilation of surface observations is done over the period from (t_o-3) to t_o hours. After t_o, instead of an immediate cessation of the assimilation by assigning 0 values to C_n, the values are gradually decreased exponentially as exp(-kt), where k is an empirical coefficient and t is the time after t_o.

4.5 Forecast Method

The BFM consists of primitive equations for winds, potential temperature, the mixing ratios of water vapor and cloud water, turbulent kinetic energy, and the turbulent length scale. These equations include second-moment representation of the heat, moisture, momentum and other fluxes, the closures of which are based on assumptions about the relation between higher order moments and known lower order moments. Other model outputs are turbulence transport coefficients of eddy viscosity and eddy diffusivity which are obtained diagnostically given the values of the above-mentioned predicted variables.

The BFM can be used for general flow and stratification conditions since its turbulence parameterization is more advanced than those used in simple eddy

viscosity models. Furthermore, when combined with a statistical cloud model, it can simulate the interactions between changes in water phase and the model dynamics. The effects of short- and long-wave radiation and topography are included in the model. At the ground, temperature is computed from an energy balance equation imposed there; heat conduction into or out from the soil is included.

This model is hydrostatic and employs the Boussinesq approximation. Under the Boussinesq approximation, a simplified equation of state:

$$\frac{\rho'}{\bar{\rho}} = - \frac{\theta'}{\bar{\theta}} \tag{42}$$

is acceptable; hence, buoyancy forces are retained in a hydrostatic basic state. This assumption is valid when density variations from the basic state are negligible, so the local acceleration and advection terms in the vertical momentum equation must be much smaller than the acceleration due to gravity. In addition, horizontal temperature variations must not be too large. For a much more detailed discussion about the model, refer to Henmi and Dumais. [10] For the sake of brevity, only a few key model details are given here.

In order to increase the accuracy of the treatment of surface boundary conditions, the vertical coordinate system introduced in equation (1) is used. This (in conjunction with the model's handling of the pressure gradient force) has necessitated some changes from Yamada. [9] Previously, the BFM used a vertically integrated version of the geostrophic pressure gradient extending from the surface to the material top of the model. In extending the vertical domain of the model, this assumption becomes inappropriate because it involves vertically averaging the virtual potential temperature. This is particularly true when the geostrophic component at the model top in the extended vertical domain has little or no relation to that near the ground, which is what is required in calculating winds there. Thus, the pressure gradient at about the 1-km level is used in calculating the geostrophic components for all levels beneath it down to the ground. Above 1 km, a modified treatment is employed in which geostrophic values from the objective analysis are used. In addition, the pressure gradient

formulation near the ground also takes into account the effect of the terrain; terrain effects above 1 km are assumed to be small and are therefore ignored. This process allows the large-scale geostrophic components to remain in line with the objective analysis guidance while at the same time including the important effects of terrain and surface physics on the pressure gradient force near the ground.

Some aspects of the BFM need to be considered when evaluating its application to the artillery meteorology problem and its consequent possible limitations. For example, any regional prognostic model either has time-dependent or fixed-lateral and top boundary conditions. In the case of the BFM without available NOGAPS forecasts, fixed-lateral boundary conditions are used. Otherwise, with available NOGAPS forecasts, time-dependent lateral boundary conditions obtained by linear in-time interpolation of the objective analysis end points are used. Currently, the time interval between NOGAPS forecasts is 12 h, so, for example, the BFM lateral boundary condition might involve both the 12- and 24-h NOGAPS forecasts at the lateral boundary location if the BFM were initialized in that 12-h period.

With a small domain, as is the case with the CAAM (BFM), the lateral boundary condition can rapidly dominate the conditions in the prognostic domain. An accurate in-time lateral boundary is thus imperative to the forecasts. Currently, the CAAM lateral boundary can lack the necessary accuracy due to the poor temporal and spatial resolution of the NOGAPS data available to CAAM. Another aspect is the treatment of terrain in proximity to the lateral boundaries. In the current BFM application, the effect of the terrain gradient on the horizontal wind is smoothed in a 5-grid-point-wide strip around the computational domain beginning at the lateral boundary and extending inward. The amount of smoothing decreases linearly from the lateral boundary, going to zero at the fifth grid point inward from the lateral boundary. This is done to prevent nonmet interactions at the lateral boundary from corrupting the forecast in the model domain. A potential problem with CAAM is that the model is set up with the potential for a small or narrow AOP; therefore, a majority of the CAAM domain could be affected by this procedure.

The final aspect is the geostrophic pressure gradient mentioned above. This is derived from the NOGAPS data and so also lacks temporal and spatial resolution.

With a strong pressure gradient, the geostrophic pressure gradient apparently dominates local forcing, but because it is derived from the NOGAPS data, it does not include mesoscale forcing.

5. Interpolation of Output Fields

The results of the CAAM modeling sequences discussed so far are gridded fields of output: a gridded forecast field of several parameters valid at the start of the run and at each of the forecast hours, and an objective analysis field valid primarily at the start of the run. The forecast field has the vertical limitations of the BFM. The analysis field is limited by the data. The CAAM products (met messages, see below) must be derived from these gridded data.

Two messages are produced for every gun and target combination of interest or for each "gun area" and "target area" combination (called sectors) identified. The first message is intended as guidance for aiming the artillery and is called a computer met message (MET-CM). The second is guidance for releasing target area munitions and is called the target area low level met message (MET-TALL).

5.1 MET-CM

The MET-CM is a formatted message containing a header for time and location and then 27 levels of met data. These data consist of level, wind direction, wind speed, virtual temperature, and pressure. The pressure is considered to be valid at the midpoint of the layer, and the other variables are layer averages. The levels range from the surface to 20 km above ground.

The data for the MET-CM are obtained from the forecast fields by first selecting the proper forecast hour's output. The data from this set of fields are first interpolated to the proper location, which is the midpoint between the gun and target. The data are then interpolated to the proper altitudes for the MET-CM. Above the highest level of the forecast fields, the objective analysis data are similarly interpolated, and the values at the highest level output from the forecast model are compared to the same level as output by the objective analysis. The difference between these values is blended with all the objective analysis data to provide values to the MET-CM levels above the forecast model. Above the top of the objective analysis data, the remaining values are provided by the standard atmosphere by using standard atmosphere lapse rates to provide temperatures and then computing pressures through the hypsometric equation. The wind direction

is assumed to remain constant, and the wind speed is assumed to approach zero in an exponential decay.

5.2 MET-TALL

The MET-TALL is similar to the MET-CM, except it is valid at the target. The MET-TALL header contains the following weather forecast parameters: cloud-base height, precipitation rate, precipitation type, and the atmosphere's electronic index of refraction. The 26 levels of data following the header have a much lower vertical extent (5 km). The data in each level consists of wind speed and wind direction, as in the MET-CM, and the other values are atmospheric temperature (not virtual) and relative humidity. These values should be valid at the midpoint of each layer (not averaged). Interpolations are carried out just as in the MET-CM, but there is little chance that blending will be required for the low levels required.

6. Discussion

6.1 Review

This report has described the CAAM (BFM) system in terms of the met modeling contained in it. There was no discussion of the user interface, the file system, nor the internal management required to manage the multiple tasks operating to perform the modeling.

The report has concentrated on the characteristics of the BFM, which is a mesoscale atmospheric prediction model and is central to the met processing. The discussion of the model domain included the issues of an AOP, horizontal grids, terrain data, and input met data. The 3DOBJ section discussed the analysis methods with and without large-scale forecast model input. The section on the BFM addressed the initialization of the model, the method used to force the model toward initialization data, and the BFM forecast technique. Finally, the output was described in terms of the met messages required by the artillery, and how they are generated from both the BFM and the 3DOBJ data.

The CAAM (BFM) system is designed to run with or without connection to the centralized weather information available through IMETS. With connection to IMETS, CAAM (BFM) utilizes the forecasts from large-scale prediction models and from openly reported upper-air soundings. With or without connection to IMETS, CAAM (BFM) always uses locally available soundings, profiler data, and satellite soundings. In its most degraded form, CAAM (BFM) will operate (although not optimally) with one local sounding. The only other requirement for operation is to have a set of DTED CD-ROMs (for terrain elevations) for the geographic area of interest.

6.2 Future Developments

This report is the first of two on the CAAM (BFM) system. The second report is planned as an in-depth verification of CAAM using real-world weather data and ballistic simulation model output. Until the verification work is completed, it is difficult to pinpoint the weaknesses of CAAM, but even without the verification

work several possible improvements to the CAAM (BFM) system appear necessary.

Better results can be expected with an improved 3DOBJ. Making large-scale forecast model data available at levels higher than 200 mb would improve the objective analysis method using forecast fields. Also, a more accurate method of using the asynoptic data is required. The current method uses the asynoptic data, but only corrects the large-scale forecast fields with an average difference.

There are two possible updates to the BFM. First, the prognostic model component of the BFM/HOTMAC lacks a stratospheric forecast capability which is needed to reach the heights required by long-range artillery. This appears to be a communication problem: NOGAPS already produces forecasts up to the 10-mb level; however, only the forecast fields up to the 200 mb level are provided by IMETS. In addition, NOGAPS forecasts are made on a 1° latitude by 1° longitude grid at 14 vertical levels, but IMETS provides only interpolated NOGAPS fields at a 2.5° latitude and longitude spacing at 6 vertical levels. Second, the HOTMAC model is preferred because of its capability to rapidly make forecasts on desktop computers. However, in so doing, its forecast accuracy is sacrificed (particularly in developing small-scale phenomena and interactions in complex terrain) because of considerable reliance on larger scale model forecasts. HOTMAC forecasts should improve as finer horizontal and vertical resolutions from the large-scale models are made available.

Additional forecast modules are being studied for addition to the CAAM (BFM) system in order to improve the capability to forecast for the target area. These might be driven implicitly by BFM output or explicitly with additional BFM prognostic variables to yield forecasts of clouds, precipitation rate and type, turbulence and visibility.

The output of met messages is based on current battlefield artillery requirements. As requirements change, the output of CAAM could also change. Specifically, with gridded forecast output, it is possible to provide met parameters along the simulated trajectory of a projectile for the purpose of producing more accurate fire-control solutions. This addition would provide improvement in those circumstances where the winds and temperature at the gun location (for example,

in a valley), differ significantly from those along the trajectory (for example, flow over mountains) and those at the target (for example, on the plains).

References

1. Blanco, A. J., "Characterizing the Measured Performance of CAAM," *Proceedings of the 1994 Battlefield Atmospherics Conference*, pp. 231-243, 1994.

2. Blanco, A., E. Vidal and S. D'Arcy, "Time and Space Weighted Computer Assisted Artillery Message," *Proceedings of the 1993 Battlefield Atmospherics Conference*, pp. 525-543, 1993.

3. Blanco, A., J. B. Spalding, and N. H. Kilmer, "Analysis of the Computer-Assisted Artillery Meteorology (CAAM) Results from a Live-Fire Exercise," Army Research Laboratory, WSMR, NM, ARL-TR-1000, 1996.

4. Spalding, J. B., N. G. Kellner, and R. S. Bonner, "Computer-Assisted Artillery Meteorology System Design," *Proceedings of the 1993 Battlefield Atmospherics Conference*, pp. 45-54, 1993.

5. Caracena, F., "Analytic Approximation of Discrete Field Samples with Weighted Sums and the Gridless Computation of Field Derivatives," *J. Atmos. Sci.*, **44**, pp. 3753-3768, 1987.

6. Barnes, S. L., "A Technique for Maximizing Details in Numerical Weather Map Analysis," *J. Appl. Meteor.*, **3**, pp. 396-409, 1964.

7. Caracena, F., "The Use of Analytic Approximations in Providing Meteorological Data for Artillery," *Proceedings of the 1992 Battlefield Atmospherics Conference*, pp. 189-198, 1992.

8. Yamada, T. and T. Henmi, "Four-Dimensional Assimilation of Large Scale Flow Field into Mesoscale Model," *Proceedings of 1993 Spring Meeting of Japan Meteorological Society,* 1993.

9. Yamada, T. and S. Bunker, "Numerical Study of Nocturnal Drainage Flows with Strong Wind and Temperature Gradients," *J. Appl. Meteor.*, **28**, pp. 545-554, 1989.

10. Henmi, T. and R. E. Dumais, "Description of the Battlescale Forecast Model," Army Research Laboratory, WSMR, NM, ARL-TR-1032, 1996.

Acronyms and Abbreviations

ARL	Army Research Laboratory
3DOBJ	three-dimensional objective analysis
AFGWC	Air Force Global Weather Central
AOP	Area of Operations
BFM	Battlescale Forecast Model
CAAM	Computer-Assisted Artillery Meteorology
DTED	Digital Terrain Elevation Data
FLOT	Forward Line of Own Troops
HOTMAC	Higher Order Turbulence Model of Atmospheric Circulation
IMETS	Integrated Meteorological System
MDS	Meteorological Data System
met	meteorological
MET-CM	computer met message
MET-TALL	target area low level met message
MPS	Mobile Profiler System
NOGAPS	Naval Operational Global Prediction System
RAOB	rawinsonde (radio wind sounding) observation
TSW	Time-Space Weighted model
WSMR	White Sands Missile Range

Distribution

	Copies
NASA MARSHAL SPACE FLT CTR ATMOSPHERIC SCIENCES DIV E501 ATTN DR FICHTL HUNTSVILLE AL 35802	1
NASA SPACE FLT CTR ATMOSPHERIC SCIENCES DIV CODE ED 41 1 HUNTSVILLE AL 35812	1
ARMY STRAT DEFNS CMND CSSD SL L ATTN DR LILLY PO BOX 1500 HUNTSVILLE AL 35807-3801	1
ARMY MISSILE CMND AMSMI RD AC AD ATTN DR PETERSON REDSTONE ARSENAL AL 35898-5242	1
ARMY MISSILE CMND AMSMI RD AS SS ATTN MR H F ANDERSON REDSTONE ARSENAL AL 35898-5253	1
ARMY MISSILE CMND AMSMI RD AS SS ATTN MR B WILLIAMS REDSTONE ARSENAL AL 35898-5253	1
ARMY MISSILE CMND AMSMI RD DE SE ATTN MR GORDON LILL JR REDSTONE ARSENAL AL 35898-5245	1
ARMY MISSILE CMND REDSTONE SCI INFO CTR AMSMI RD CS R DOC REDSTONE ARSENAL AL 35898-5241	1

ARMY MISSILE CMND
AMSMI
REDSTONE ARSENAL AL 35898-5253 1

CMD (420000D(C0245))
ATTN DR A SHLANTA
NAVAIRWARCENWPNDIV
1 ADMIN CIR
CHINA LAKE CA 93555-6001 1

PACIFIC MISSILE TEST CTR
GEOPHYSICS DIV
ATTN CODE 3250
POINT MUGU CA 93042-5000 1

NAVAL OCEAN SYST CTR
CODE 54
ATTN DR RICHTER
SAN DIEGO CA 52152-5000 1

METEOROLOGIST IN CHARGE
KWAJALEIN MISSILE RANGE
PO BOX 67
APO SAN FRANCISCO CA-96555 1

DEPT OF COMMERCE CTR
MOUNTAIN ADMINISTRATION
SPPRT CTR LIBRARY R 51
325 S BROADWAY
BOULDER CO 80303 1

DR HANS J LIEBE
NTIA ITS S 3
325 S BROADWAY
BOULDER CO 80303 1

NCAR LIBRARY SERIALS
NATL CTR FOR ATMOS RSCH
PO BOX 3000
BOULDER CO 80307-3000 1

DEPT OF COMMERCE CTR
325 S BROADWAY
BOULDER CO 80303 1

DAMI POI
WASHINGTON DC 20310-1067 1

MIL ASST FOR ENV SCI OFC
OF THE UNDERSEC OF DEFNS
FOR RSCH & ENGR R&AT E LS
PENTAGON ROOM 3D129
WASHINGTON DC 20301-3080 1

DEAN RMD
ATTN DR GOMEZ
WASHINGTON DC 20314 1

ARMY INFANTRY
ATSH CD CS OR
ATTN DR E DUTOIT
FT BENNING GA 30905-5090 1

AIR WEATHER SERVICE
TECH LIBRARY FL4414 3
SCOTT AFB IL 62225-5458 1

USAFETAC DNE
ATTN MR GLAUBER
SCOTT AFB IL 62225-5008 1

HQ AWS DOO 1
SCOTT AFB IL 62225-5008 1

PHILLIPS LABORATORY
PL LYP
ATTN MR CHISHOLM
HANSCOM AFB MA 01731-5000 1

ATMOSPHERIC SCI DIV
GEOPHYISCS DIRCTRT
PHILLIPS LABORATORY
HANSCOM AFB MA 01731-5000 1

PHILLIPS LABORATORY
PL LYP 3
HANSCOM AFB MA 01731-5000 1

ARMY MATERIEL SYST
ANALYSIS ACTIVITY
AMXSY
ATTN MR H COHEN
APG MD 21005-5071 1

ARMY MATERIEL SYST
ANALYSIS ACTIVITY
AMXSY AT
ATTN MR CAMPBELL
APG MD 21005-5071 1

ARMY MATERIEL SYST
ANALYSIS ACTIVITY
AMXSY CR
ATTN MR MARCHET
APG MD 21005-5071 1

ARL CHEMICAL BIOLOGY
NUC EFFECTS DIV
AMSRL SL CO
APG MD 21010-5423 1

ARMY MATERIEL SYST
ANALYSIS ACTIVITY
AMSXY
APG MD 21005-5071 1

ARMY MATERIEL SYST
ANALYSIS ACTIVITY
AMXSY CS
ATTN MR BRADLEY
APG MD 21005-5071 1

ARMY RESEARCH LABORATORY
AMSRL D
2800 POWDER MILL ROAD
ADELPHI MD 20783-1145 1

ARMY RESEARCH LABORATORY
AMSRL OP SD TP
TECHNICAL PUBLISHING
2800 POWDER MILL ROAD
ADELPHI MD 20783-1145 1

ARMY RESEARCH LABORATORY
AMSRL OP CI SD TL
2800 POWDER MILL ROAD
ADELPHI MD 20783-1145 1

ARMY RESEARCH LABORATORY 1
AMSRL SS SH
ATTN DR SZTANKAY
2800 POWDER MILL ROAD
ADELPHI MD 20783-1145

ARMY RESEARCH LABORATORY 1
AMSRL
2800 POWDER MILL ROAD
ADLEPHI MD 20783-1145

NATIONAL SECURITY AGCY W21 1
ATTN DR LONGBOTHUM
9800 SAVAGE ROAD
FT GEORGE G MEADE MD 20755-6000

OIC NAVSWC 1
TECH LIBRARY CODE E 232
SILVER SPRINGS MD 20903-5000

ARMY RSRC OFC 1
ATTN AMXRO GS (DR BACH)
PO BOX 12211
RTP NC 27009

DR JERRY DAVIS 1
NCSU
PO BOX 8208
RALEIGH NC 27650-8208

US ARMY CECRL 1
CECRL GP
ATTN DR DETSCH
HANOVER NH 03755-1290

ARMY ARDEC 1
SMCAR IMI I BLDG 59
DOVER NJ 07806-5000

ARMY SATELLITE COMM AGCY 1
DRCPM SC 3
FT MONMOUTH NJ 07703-5303

ARMY COMMUNICATIONS 1
ELECTR CTR FOR EW RSTA
AMSEL EW D
FT MONMOUTH NJ 07703-5303

ARMY COMMUNICATIONS
ELECTR CTR FOR EW RSTA
AMSEL EW MD
FT MONMOUTH NJ 07703-5303 1

ARMY DUGWAY PROVING GRD
STEDP MT DA L 3
DUGWAY UT 84022-5000 1

ARMY DUGWAY PROVING GRD
STEDP MT M
ATTN MR BOWERS
DUGWAY UT 84022-5000 1

DEPT OF THE AIR FORCE
OL A 2D WEATHER SQUAD MAC
HOLLOMAN AFB NM 88330-5000 1

PL WE
KIRTLAND AFB NM 87118-6008 1

USAF ROME LAB TECH
CORRIDOR W STE 262 RL SUL
26 ELECTR PKWY BLD 106
GRIFFISS AFB NY 13441-4514 1

AFMC DOW
WRIGHT PATTERSON AFB OH 45433-5000 1

ARMY FIELD ARTILLERY SCHOOL
ATSF TSM TA
FT SILL OK 73503-5600 1

NAVAL AIR DEV CTR
CODE 5012
ATTN AL SALIK
WARMINISTER PA 18974 1

ARMY FOREIGN SCI TECH CTR
CM
220 7TH STREET NE
CHARLOTTESVILLE VA 22448-5000 1

NAVAL SURFACE WEAPONS CTR
CODE G63
DAHLGREN VA 22448-5000 1

ARMY OEC
CSTE EFS
PARK CENTER IV
4501 FORD AVE
ALEXANDRIA VA 22302-1458 1

ARMY CORPS OF ENGRS
ENGR TOPOGRAPHICS LAB
ETL GS LB
FT BELVOIR VA 22060 1

ARMY TOPO ENGR CTR
CETEC ZC 1
FT BELVOIR VA 22060-5546 1

SCI AND TECHNOLOGY
101 RESEARCH DRIVE
HAMPTON VA 23666-1340 1

ARMY NUCLEAR CML AGCY
MONA ZB BLDG 2073
SPRINGFIELD VA 22150-3198 1

USATRADOC
ATCD FA
FT MONROE VA 23651-5170 1

ARMY TRADOC ANALYSIS CTR
ATRC WSS R
WSMR NM 88002-5502 1

ARMY RESEARCH LABORATORY
AMSRL BE S
BATTLEFIELD ENVIR DIR
WSMR NM 88002-5501 1

ARMY RESEARCH LABORATORY
AMSRL BE E
BATTLEFIELD ENVIR DIR
WSMR NM 88002-5501 1 1

ARMY RESEARCH LABORATORY
AMSRL BE W
BATTLEFIELD ENVIR DIR
WSMR NM 88002-5501 1

DTIC
8725 JOHN J KINGMAN RD
STE 0944
FT BELVOIR VA 22060-6218 1

ARMY MISSILE CMND
AMSMI
REDSTONE ARSENAL AL 35898-5243 1

ARMY DUGWAY PROVING GRD
STEDP3
DUGWAY UT 84022-5000 1

USTRADOC
ATCD FA
FT MONROE VA 23651-5170 1

WSMR TECH LIBRARY BR
STEWS IM IT
WSMR NM 88001 1

US MILITARY ACADEMY
MATHEMATICAL SCI CTR EXCELLENCE
DEPT OF MATHEMATICAL SCIENCES
ATTN MDN A (MAJ DON ENGEN)
THAYER HALL
WEST POINT NY 10996-1786 1

PATRICK A HAINES
ARTILLERY METEOROLOGY BRANCH
ARMY RESEARCH LABORATORY
WSMR NM 88002 10

ABEL J BLANCO
ARTILLERY METEOROLOGY BRANCH
ARMY RESEARCH LABORATORY
WSMR NM 88002 10

S A LUCES
PHYSICAL SCIENCE LABORATORY
NEW MEXICO STATE UNIVERSITY
LAS CRUCES NM 88003 5

JOHN B SPALDING
PHYSICAL SCIENCE LABORATORY
NEW MEXICO STATE UNIVERSITY
LAS CRUCES NM 88003 5

ARMAMENT RESEARCH DEVELOPMENT AND ENGINEERING CENTER FIRING TABLES AND AEROBALLISTICS BRANCH ATTN ROBERT LIESKE ABERDEEN PROVING GROUND MD 21005-5059	1
CHARLES A CLOUGH US ARMY TEST CENTER ATTN STEAC-EN-M BLDG 1134 ABERDEEN PROVING GROUND MD 21005-5059	1
Record Copy	1
TOTAL	109